

Population Data Spatial Analysis in the Border Area of Shanxi, Hebei and Inner Mongolia in China

Jianming Yu and Yuan Ma

Inner Mongolia Earthquake Administration, Hohhot, China

Email: {vs820, mayuanreceive}@foxmail.com

Abstract—Spatialization of population statistics is an effective way to solve the problem of data fusion between statistics and natural factors. In order to solve the problems of data aging and inadequate spatial precision of population data in Inner Mongolia Bureau, this study used NPP/VIIRS night light data, residential population statistics and land use data as data sources, and selected appropriate models to simulate population spatial distribution at county level in the border area of Shanxi, Hebei and Mongolia. Based on land use data, a stepwise regression model is established to generate spatialized population data of each county in the border area, and then the accuracy of the evaluation data is tested with the standard of resident population statistics. Finally, the goal of the transformation of population statistics from administrative divisions to kilometer grids is realized.

Index Terms—data spatialization, nighttime light, progressive regression, zonal modeling

I. SURVEY OF THE RESEARCH AREA

The zone in Inner Mongolia of the border area has a total area of about 17,000 km² [1], including Jining District, Fengzhen City, Zhuozi County, Chahar Right Front Banner, Liangcheng County, Xinghe County, Horlinger County and Qingshuihe County in Hohhot City, as shown in Fig. 1. The area has been designated as a seismic risk area for many years. There are many active faults since the Late Pleistocene, which have the tectonic background of strong earthquakes and the rupture gap of historical earthquakes. As one of the most important population habitats in North China, there exists natural disasters such as earthquakes, debris flows and landslides frequently. In addition, the complex topographic and geomorphological conditions in this area have resulted in the prominent contradiction between man and land. Therefore, the study of population distribution in the border area can provide technical support for coordinated and stable economic development, disaster risk assessment and rescue.

II. DATA SOURCES AND PREPROCESSING

All data of the study listed in detail are shown in Table I, VIIRS Day/Night Band Nighttime Lights data and land

use data will be cut, resampled and projected with the unified geographic reference of WGS-84 ellipsoid and Albers isoconic projection (the central longitude is 105°E, the double standard latitudes are 25°N and 47°N, respectively, and the starting point is 0°N).

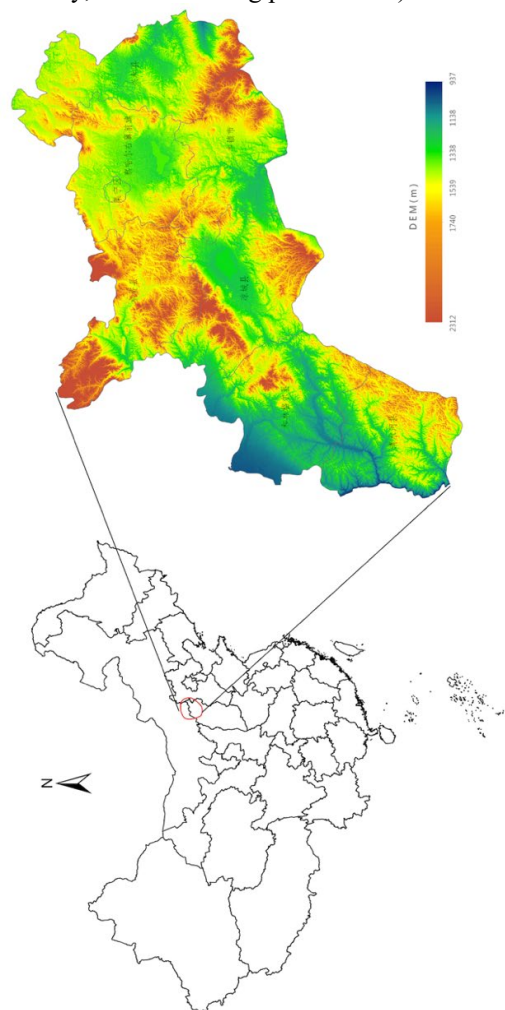


Figure 1. Location and elevation distribution of the border area in Shanxi, Hebei and Inner Mongolia (Inner Mongolia part).

1) VIIRS day/night band nighttime lights data

On October 28, 2011, the first satellite of the National Polar-orbiting Operational Environmental Satellite System Preparatory Project, Suomi NPP, was launched.

NPP carried the Visible Infrared Imag in five earth observation instruments. Radiometer Suite (VIIRS) has 22 bands, 5 image bands with resolution of 375 m, one DNB band with resolution of 500 m, and 16 visible and infrared channels with resolution of 750 M. Among them, the DNB band gray scale interval (14bit) can detect even weaker light sources, so it can be applied in the fields of atmospheric, land surface change process and human surface activity [2].

The Nighttime Lights data is released monthly as the synthetic product, which has been updated to April 2019. The study used the average nighttime lights image of 2016, with downloading URL: www.ngdc.noaa.gov/eog/viirs/download_dnb_composites.html, as shown in Fig. 2.

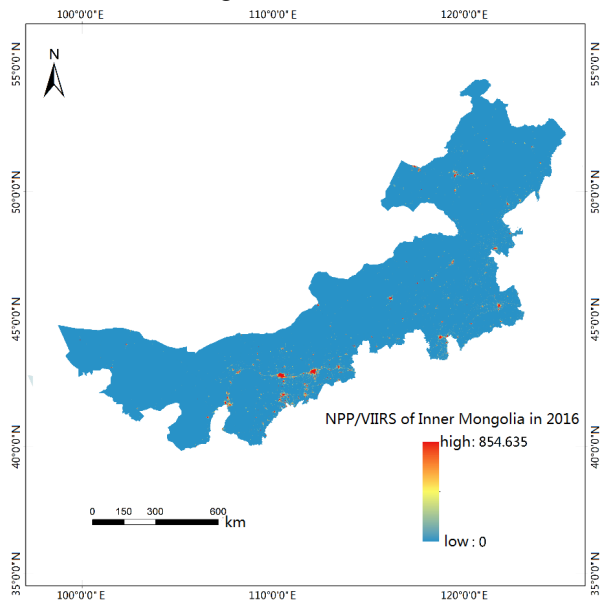


Figure 2. VIIRS day/night band nighttime lights data of Inner Mongolia in 2016.

Data preprocessing mainly includes two aspects: synthesis and noise removal of NPP/VIIRS Nighttime Lights monthly data. At present, the annual average method and the annual maximum method [3] are widely used for data synthesis.

The annual maximum method:

$$M_R = \text{Max}(R_1, R_2, R_3, \dots) \quad (1)$$

The annual average method:

$$A_R = \text{Average}(R_1, R_2, R_3, \dots) \quad (2)$$

In formulas (1) and (2), M_R , A_R and R_i represent the maximum nighttime lights reflectance, the average nighttime lights reflectance and the nighttime lights reflectance of i th month, respectively. In order to eliminate errors due to June data loss and short-term lights data [4], the study chooses the average method to merge 11-month lights products to obtain NPP/VIIRS nighttime lights data of Chinese Mainland in 2016.

The original nighttime lights data is first extracted based on the mask of area with non-zero gray value and then processed using threshold method to remove background noise. The maximum of nighttime lights data

of four major cities, Hohhot, Baotou, Ordos and Ulanqab, is selected as the threshold of nighttime lights in the Shanxi-Hebei-Inner Mongolia border area.

From Fig. 3 it can be seen that the ranking of maximum nighttime lights in these four cities is: Ordos City, Baotou City, Hohhot City, Ulanqab City. Then as the maximum threshold for Nighttime Lights data, V_{max} is smoothed using eight neighborhood method.

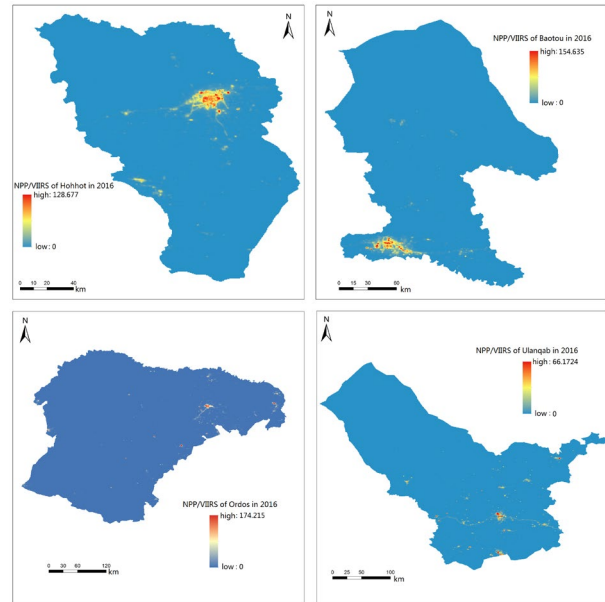


Figure 3. VIIRS day/night band nighttime lights data of four major Cities (Hohhot, Baotou, Ordos and Ulanqab) in 2016.

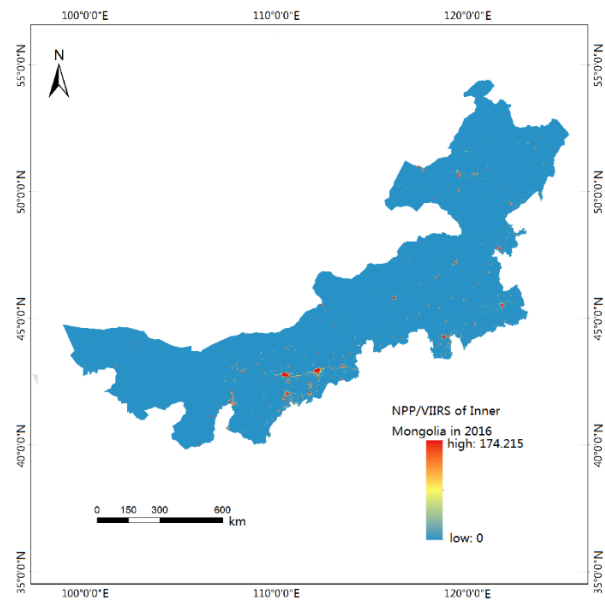


Figure 4. VIIRS day/night band nighttime lights correction data of Inner Mongolia in 2016.

Eight neighborhood method [5]: if the light value of the central pixel is greater than the threshold value, the maximum light value of all the pixels in the eight neighbors around the pixel is searched, and if the value is less than the threshold value, it is assigned to the central pixel. Cycle the above process until the maximum pixel value less than the threshold around the central pixel is

found, and assign it to the central pixel, then slide the window in turn to complete the whole image processing, as shown in Fig. 4. This method can effectively remove the short-term light data from NPP/VIIRS nighttime lights data.

2) Demographic statistics

Population data are the resident population statistics in census data, mainly from the statistical yearbook and the statistics bulletin of the autonomous region government in 2017. Statistical data of permanent population are connected with corresponding administrative boundaries according to administrative division codes, then the vector population spatial database of all levels (provinces, cities and counties) is obtained as shown in the Fig. 5 and Fig. 6.

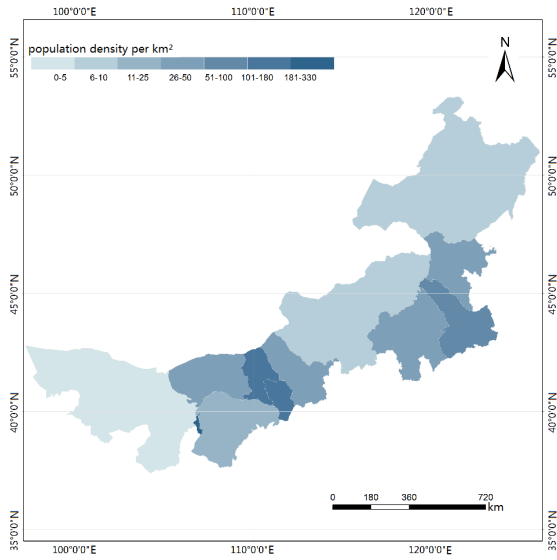


Figure 5. Spatial distribution map of resident population density in prefecture level cities of Inner Mongolia in 2016.

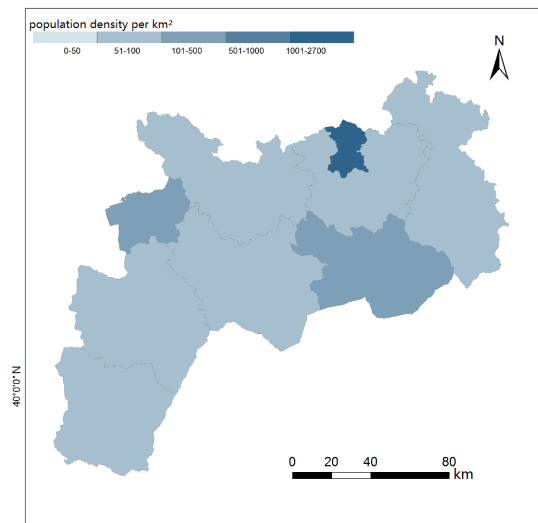


Figure 6. Spatial distribution map of resident population density in counties of the border areas in 2016.

3) Data of administrative divisions

The data of administrative divisions are from the basic database of the Emergency Response Center of China

Earthquake Administration, including provincial, municipal and county administrative divisions, collected in 2019 with the proportion of 1:250,000.

4) Land use data

Land use data are from Institute of Geographic Sciences and Natural Resources, Chinese Academy of Sciences, collected in 2015. The data set divides land use/cover into six primary types, including arable land, woodland, grassland, water area, construction land and unused land, and 22 secondary types shown in Fig. 7, including woodland, shrub forest, sparse woodland, other woodland, high, medium and Low-covered grassland and so on.

In the study, 1 km resolution vector land use data in the border area will be converted into 1 km auxiliary raster data using the Polygon to Raster Tool in ArcGIS desktop.

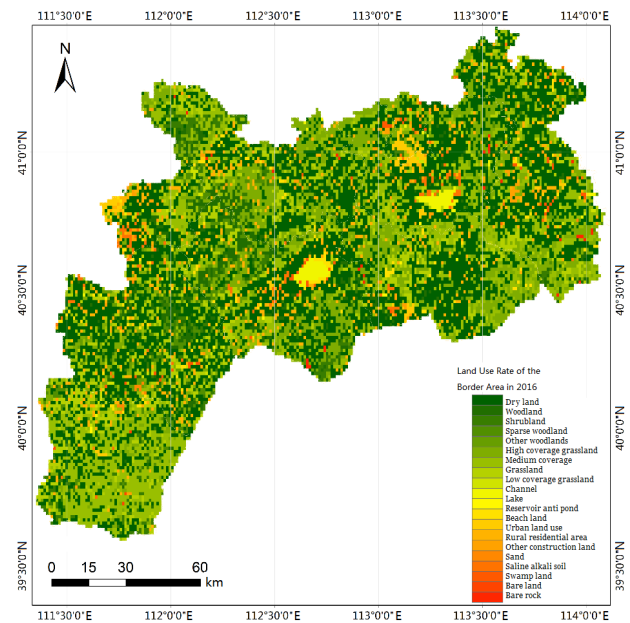


Figure 7. 1 km resolution land use map of the border area (Inner Mongolia part) in 2015.

III. RESEARCH METHODS AND ACCURACY VERIFYING

A. Regression Fitting

In this study, three types of regression fitting methods, including linear regression, polynomial regression and power function regression, are used to analyze the population scale suitability simulated by two kinds of nighttime data:

TABLE I. DATA SOURCE

Data Type	Time	Data Source	Scale/Resolution
Administrative Division	2019	Emergency Response Center of CEA	1:250000
Demographic Data	2017	Statistical Yearbook of Inner Mongolia Autonomous Region	provincial, municipal, county and town
LUC	2015	Geographic Sciences and Natural Resources, CAS	1 km
NPP/VIIRS	2016	NOAA	0.5 km

linear regression: $P=a \times NTL+b$,

polynomial regression: $P=a \times NTL^2+b \times NTL+c$,

power function regression: $P=a \times NTL^b$,

In the formula above: P represents demographic data based on administrative units, NTL represents the nighttime light index in administrative units, and a , b and c are the model coefficients. In this study uses these models will be used to fit the population and nighttime light data on scales of provinces, cities and counties.

B. Stepwise Regression Analysis

The principle of stepwise regression modeling method is that all introduced variables are sorted in order according to the contribution degree of each variable to the dependent variable, in which the contribution degree is to calculate the sum of the partial regression squares of each variable, and then select the variable with the least sum of the partial regression squares for significance test. If the variable is significant at the given confidence level, the change need not be eliminated. Quantity and other variables do not need to be excluded. On the contrary, if it does not pass the significance test of the set confidence level, it needs to be deleted. The remaining variables are tested according to the contribution degree. Only the variables passing the significance test are retained. Then the partial square sum of the independent variables which are not introduced into the equation is calculated, and one of the independent variables with the greatest contribution degree is selected. Variables are tested for significance at a given confidence level. If significant, the independent variable is retained and the process is repeated until no independent variable is introduced into the equation and no independent variable is removed from the equation. Thus the final regression equation is the optimal stepwise regression equation [6].

C. Accuracy Evaluation Method

Five factors, namely, correlation coefficient (R), root mean square error (RMSE), mean absolute error (MAE), mean relative error (MRE) and relative error (RE), are selected for the accuracy evaluation and error analysis of the simulated population.

1) Coefficient of correlation

In statistics, Pearson correlation coefficient can be abbreviated as correlation coefficient (R), which is an index used to measure the linear correlation between variables X and Y [7]. The value of correlation coefficient is between - 1 and + 1, +1 means complete positive correlation and -1 means complete negative correlation. The concrete calculation formula is as follows:

$$R = \frac{\sum_{i=1}^n (P_i - \bar{P})(PE_i - \overline{PE})}{\sqrt{\sum_{i=1}^n (P_i - \bar{P})^2} \sqrt{\sum_{i=1}^n (PE_i - \overline{PE})^2}} \quad (3)$$

P_i and PE_i represent the statistical and estimated population in the i th administrative unit, respectively, n represents the number of administrative units, \bar{P} and

\overline{PE} represents the average statistical and estimated population, respectively.

2) RMS error

RMS error is used to measure the deviation between the estimated value and the actual value, which could well reflect the accuracy of the simulation results, and can also be used to measure the prediction ability of the model [8]. The calculation formula is as follows:

$$RMSE = \sqrt{\frac{\sum_{i=1}^n (PE_i - P_i)^2}{n}} \quad (4)$$

P_i and PE_i represent the statistical and estimated population in the i th administrative unit, respectively, n represents the number of administrative units. The smaller the RMS error is, the higher the accuracy of the estimation results is.

3) Mean absolute error

MAE is used to measure the proximity between estimated and measured values [9]. The calculation formula is as follows:

$$MAE = \frac{1}{n} \sum_{i=1}^n |PE_i - P_i| \quad (5)$$

P_i and PE_i represent the statistical and estimated population in the i th administrative unit, respectively, n represents the number of administrative units. The larger the MAE is, the farther the deviation between the estimated and the actual value is.

4) Mean relative error

The MRE can be used to quantitatively reflect the average oscillation amplitude of the deviation between the estimated and the measured value [10]. The calculation formula is as follows:

$$MRE = \frac{1}{n} \sum_{i=1}^n \frac{|PE_i - P_i|}{P_i} \quad (6)$$

P_i and PE_i represent the statistical and estimated population in the i th administrative unit, respectively, n represents the number of administrative units. The larger the MRE is, the farther the deviation between the estimated and the actual value is.

5) Relative error

$$RE_i = \frac{PE_i - P_i}{P_i} \quad (7)$$

P_i and PE_i represent the statistical and estimated population in the i th administrative unit, respectively, n represents the number of administrative units. The relative errors are classified according to the following criteria of Table II [11]:

TABLE II. RELATIVE ERROR CLASSIFICATION CRITERIA

Relative Error Range	Classification
< -50%	Serious Underestimation
-50% ~ -25%	General Underestimation
-25% ~ 25%	More Accurate Estimation
25% ~ 50%	General Overestimation
> 50%	Serious Overestimation

IV. POPULATION SIMULATING RESULTS ADDING OTHER AUXILIARY DATA

We will get a low population simulation accuracy when just based on individual nighttime light data in the small size of the demographic unit. Based on this understanding, considering the advantages of NPP/VIIRS in simulating population at county level and the characteristics of land use types of the study area, nighttime light data and LUCC are combined to take error analyzing using stepwise regression analysis fitting model at the township scale [12].

A. Data Characteristics of Land Use Types

The land use spatial distribution of the border areas of Shanxi, Hebei and Mongolia in 2015 is shown in Fig. 8, that is, the first-class land use and cover types, including woodland, cultivated land, water area, grassland, urban and rural industrial and mining residential land and unused land.

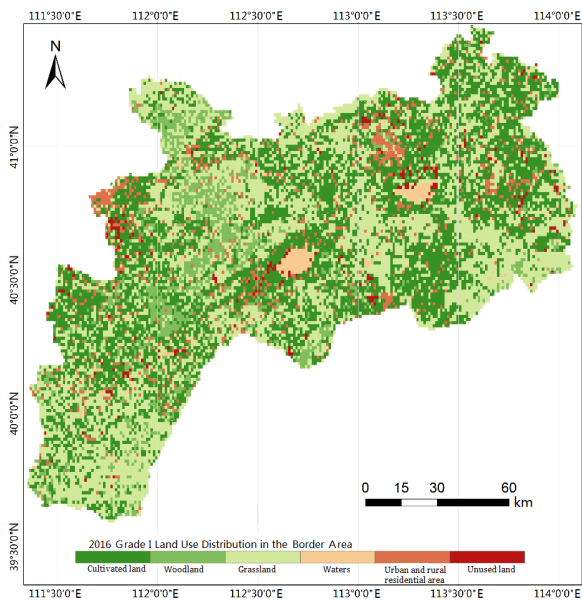


Figure 8. The first class spatial distribution map of land use classification of the border area in 2016.

There are 7045 km² grassland, 6864 km² cultivated land and 1670 km² woodland in the border area, and the distribution of which is closely related to the topography. There are 117 km² of urban and rural areas, industrial and mining areas and construction land, mainly concentrated in Hohhot and Ulanqab cities and their surrounding districts and counties. Further, through the statistics of land use area in the border area as shown in Fig. 9, and the SPSS calculation of the resident population and land use cover area of each district and county, the analysis results show that land use distribution is closely related to human activities. From Table III, it is obvious that the correlation between land use data and population of each type is arable land, urban and rural industrial and mining residents in turn, the corresponding coefficients are 0.62, 0.57, -0.45, -0.44 -0.3 and 0.08, respectively. Among them, both the cultivated land and urban and rural industrial and mining residential land have significant positive correlation with population (P=0.01), while

woodland, grassland, unused land have significant negative correlation with population (P=0.01). Considering the actual population distribution situation, waters and unused land types are not involved in the process of population spatialization research with land use data.

TABLE III. THE CORRELATION ANALYSIS BETWEEN LAND USE DATA AND POPULATION OF THE BORDER AREA

Land Type	Correlation(R)	Note: * is significant at the 0.01 confidence level.
Unused Land	-0.30**	
Rural and Urban Residential Land	0.57**	
Waters	0.08**	
Grassland	-0.45**	
Woodland	-0.44**	
Cultivated Land	0.62**	

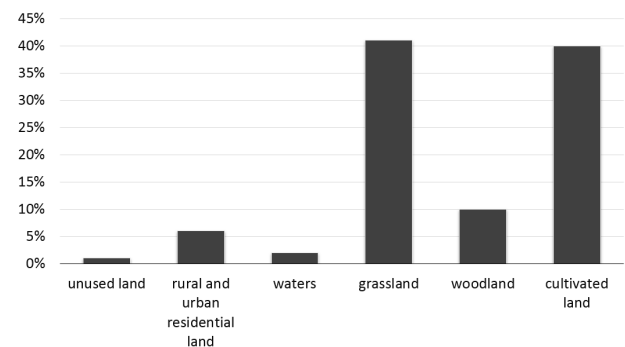


Figure 9. The proportion of land use types of the border area in 2016.

B. Population Spatialization

1) Method

Based on SPSS software, the resident population statistics of each district and county are taken as dependent variables, the pixels with brightness value of 0 in night lighting image are taken as dark elements, the pixels with brightness not equal to 0 at night are taken as bright elements, and then the number of brightness elements, dark elements and total brightness of night lighting under different land use types in each district and county are taken as independent variables to carry out stepwise regression analysis to obtain the model self-variation and regression coefficients. Finally, spatial analysis of population is carried out based on the established model [13]. Considering the complexity of the calculation process of extracting masks separately, the study adopts the grid computing method to superimpose LUCC data and night lighting data. First the kilometer grid vector data of the border area are established to calculate the corresponding land use types, bright elements, dark elements and total brightness of lights on each grid, which will be superimposed with the boundary of county administrative divisions to get the bright elements number, dark elements number and total light brightness on each land use type of each county via the method of data perspective table in EXCEL.

2) Stepwise regression modeling

The extracted model variables include: *NU* represents the pixel number of a land use type whose night light

value is 0, NL represents the pixel number of a land use type whose night light value is greater than 0, LE represents the total radiation brightness value of the light under this land use type, the confidence level of each independent variable entering the equation of the model is 0.05, and the confidence level of the rejection equation is 0.1. Although the constant of the regression equation is positive, the initial model may have negative coefficients of some independent variables [14], the main reason is the collinearity between the variables, so the model gets the population negative value which is not consistent with the actual situation. The solution is to eliminate the variables with negative coefficients directly, and then introduce the remaining variables into the model again, so that the coefficients of the independent variables entering the model and the constant are all positive. The model expression [15] is:

$$P_i = P_0 + \sum_{j=1}^M (a_j \times NU_{ij} + b_j \times NL_{ij} + c_j \times LE_{ij}) \quad (8)$$

where P_i represents the i th county statistical population, P_0 is a constant, M is the number of land types, and NU_{ij} , NL_{ij} , LE_{ij} are the number of light elements, dark elements and total brightness index of the j th land use type in the i th county, respectively. a_j , b_j , c_j are regression coefficients [16], and pixel scale population can be obtained by:

$$P_{ijk} = P_0 / N_i + \sum_{j=1}^M (a_j \times NU_{ijk} + b_j \times NL_{ijk} + c_j \times LE_{ijk}) \quad (9)$$

where P_{ijk} represents the population in the k th pixel of the j th land use type in the i th county, N_i is the pixel number of the i th county, M is the number of land types, U_{ijk} , NL_{ijk} , LE_{ijk} are light element number, dark element number and total brightness index on the k th pixel of the j th land use type in the i th county, a_j , b_j , c_j are regression coefficients.

$$P'_{ijk} = P_{ijk} \times \frac{\bar{P}_i}{P_i} \quad (10)$$

where P'_{ijk} represent the final grid population, \bar{P}_i is the statistical population of i th county, P_i represents the sum of all pixel values of the i th county.

Formula (8) is the expression of the relationship between population and light intensity of various types of land on the county unit, through which the regression coefficient of relevant variables (dark element number, light element number and light intensity of various types of land) can be obtained. Formula (9) is to carry out population estimation on the pixel scale using a calculation model with the regression coefficients obtained from formula (8). Formula (10) is to fine tune the difference between the population census data and the population spatial statistics of all the pixels on the county unit based on formula (9), so as to ensure that the population spatial distribution simulation data summarized on the county scale is consistent with the actual statistical data.

From Table IV, it can be seen that the variables in the model after superposition of night light data and land use

are the same, including the light and dark elements number of the cultivated land, the total light brightness of forest land and urban or construction land, and all above pass the significance test ($P=0.01$). There may be scattered rural residential areas, independent houses for farmers and herdsmen, boat houses, tents, yurts, and other facilities in cultivated land, forest land, grassland, even desert and water area due to the high precision of land use products interpreted by satellite remote sensing [17]. The above small, scattered but large number of residential facilities cannot be reflected in the 1:100,000 LUCC data used in this study, but they do exist. Therefore, the study gives a certain weight to the possibility of population distribution in the above land types. The modeling results show that the complex correlation coefficient of the model based on NPP/VIIRS nighttime light data and LUCC is 0.817, with a high degree of correlation.

TABLE IV. REGRESSION COEFFICIENT OF MODEL

Land Use Type		NPP/VIIRS	
		Coefficient	Sig.
Cultivated Land	NU	95.736	0.000
	NL	163.979	0.000
Forest Land	LE	85.934	0.028
Urban and Construction Land	LE	71.042	0.000
Constant	CON	45683.36	0.017
	R ²	0.817	

3) Results of population spatialization

The population spatial results of in the border area based on NPP/VIIRS nighttime light data and LUCC data are shown in Fig. 10. The population is mainly concentrated in residential areas and urban construction land, and the high population density areas of each district and county are mainly concentrated in the county seat, of which Saihan District of Hohhot City and Jining District of Ulanqab City have the most concentrated population and the highest density due to the rapid urbanization and economic development.

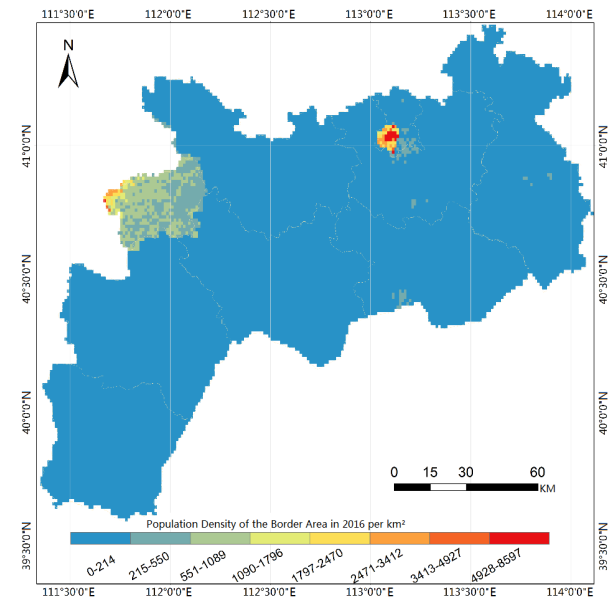


Figure 10. Population spatial distribution simulation results based on NPP/VIIRS night light data in 2016.

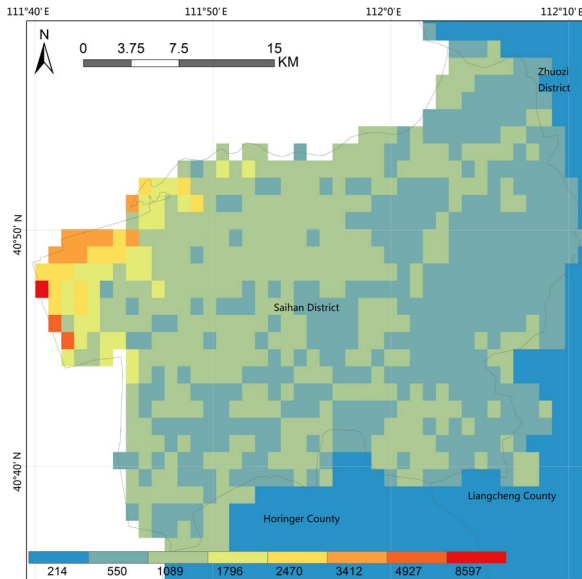


Figure 11. Spatial distribution of the most densely populated region in the border area.

Fig. 11 shows the population spatial distribution simulation in the central urban region of the border area based on NPP/VIIRS nighttime light data and LUCC data. The spatial population distribution pattern is high in the central urban region and low in the surrounding areas. Saihan district has the highest population density of more than 8500 people per square kilometer. Fig. 11 clearly depicts the population distribution within the district and county, including the change of the overall population density.

C. Accuracy Inspection

The 2016 resident population statistics data of 30 villages and towns in the border area are randomly selected as the real population data, the population spatial distribution simulation based on NPP/VIIRS nighttime light data and LUCC are used as estimate, either of them is calculated the overall Mean Absolute Error (MAE), Mean Relative Error (MRE), Root Mean Square Error (RMSE), and the population estimates of each village and town. The error is analyzed by grading statistics.

TABLE V. POPULATION SPATIALIZATION ERROR

Error Type	NPP/VIIRS	NPP/VIIRS and LUCC
MAE	11236	10450
MRE	49.35%	44.62%
RMSE	614835	587170

MAE, MRE and RMSE, based on the 2016 resident population statistics data and the population spatial distribution simulation extracted by the combination of NPP/VIIRS nighttime light data and LUCC, and only NPP/VIIRS are shown in Table V. It is found that the spatialization accuracy results based on NPP/VIIRS night light data and LUCC data is higher than that of the results using light data directly.

Table VI shows the classification statistics of the population relative errors of 30 towns, and Fig. 12 shows the relative errors proportion of each estimation level. Based on NPP/VIIRS nighttime light data, the proportion of townships with accurate spatial population estimation is 45%, which shows that the accuracy of population spatial can be greatly improved by introducing LUCC when using nighttime light data for population spatialization.

TABLE VI. RELATIVE ERROR CLASSIFICATION LIST

Nighttime Light	Relative Error Classification		
	Serious Underestimation (-100%-, -50%)	Generally Underestimated (-50%, -25%)	More Accurate Estimation (-25%, -25%)
NPP/VIIRS	2	6	13
Nighttime Light	Generally Overestimated (25%, 50%)	Severely Overestimated (50%, 100%+)	
NPP/VIIRS	4	5	

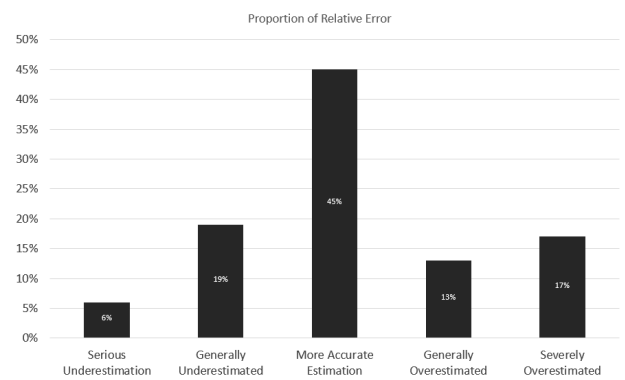


Figure 12. Relative error proportion chart.

V. CONCLUSION

The study is to spatialize the population of districts and counties in the border area in a small regional scale with other auxiliary data to improve the fitting accuracy.

First the results of correlation analyzing between the permanent population statistical data and the LUCC in the study area show that there is a significant correlation between the population and the land use type in the border area; then, and then the step-by-step regression analysis model by combining the LUCC with the NPP/VIIRS nighttime light data is carried out to obtain the 1 km (NPP/VIIRS) spatial population distribution data in the border area. Finally, 30 township population statistics data are randomly selected for precision analysis. The accuracy of the random 30 township population statistics data shows that the accuracy of the population spatial distribution data based on NPP/VIIRS nighttime light data and LUCC is higher, the overall error is smaller (including Mae, MRE and RMSE), the number of towns accurately estimated is more than that of the single nighttime light data, and the number of towns misjudged is less.

CONFLICT OF INTEREST

The authors declare no conflict of interest.

AUTHOR CONTRIBUTIONS

Jianming Yu conducted the research and wrote the paper; Yuan Ma analyzed the data and fixed the bug of the program; all authors had approved the final version.

ACKNOWLEDGMENT

This work was supported by Key Tasks for Youth in Earthquake Emergency Response of CEA under Grant No. CEA-EDEM-201904.

REFERENCE

- [1] X. Q. Wang and X. Ding, "On-site investigation report of border area of Shanxi, Hebei and Inner Mongolia in 2017," Institute of Seismic Prediction, China Seismological Bureau, 2017.
- [2] C. Lo, "Modeling the population of China using DMSP operational linescan system nighttime data," *Photogrammetric Engineering and Remote Sensing*, vol. 67, no. 9, pp. 1037-1047, 2001.
- [3] X. Yang, *et al.*, "An updating system for the gridded population database of China based on remote sensing, GIS and spatial database technologies," *Sensors*, vol. 9, no. 2, pp. 1128-1140, 2009.
- [4] T. X. Yue, *et al.*, "Surface modelling of human population distribution in China," *Ecological Modelling*, vol. 181, no. 4, pp. 461-478, 2005.
- [5] F. J. Gallego, "A population density grid of the European Union," *Population and Environment*, vol. 31, no. 6, pp. 460-473, 2010.
- [6] C. Linard, *et al.*, "Population distribution, settlement patterns and accessibility across Africa in 2010," *PLOS One*, vol. 7, no. 2, p. e31743, 2012.
- [7] M. R. Khomarudin, *et al.*, "Hazard analysis and estimation of people exposure as contribution to tsunami risk assessment in the West Coast of Sumatra, the South Coast of Java and Bali," *Zeitschrift Für Geomorphologie, Supplementary Issues*, vol. 54, no. 3, pp. 337-356, 2010.
- [8] X. Li, *et al.*, "Potential of NPP-VIIRS nighttime light imagery for modeling the regional economy of China," *Remote Sensing*, vol. 5, no. 6, pp. 3057-3081, 2013.
- [9] Y. Liao, J. Wang, B. Meng, and X. Li, "Integration of GP and GA for mapping population distribution," *International Journal of Geographical Information Science*, vol. 24, no. 1, pp. 47-67, 2010.
- [10] J. Liu, *et al.*, "Spatiotemporal characteristics, patterns, and causes of land-use changes in China since the late 1980s," *Journal of Geographical Sciences*, vol. 24, no. 2, pp. 195-210, 2014.
- [11] X. H. Liu and M. G. Kyriakidis, "Population-density estimation using regression and area-to-point residual Kriging," *International Journal of Geographical Information Science*, vol. 22, no. 4, pp. 431-447, 2008.
- [12] C. P. Lo, "Modeling the population of China using DMSP operational linescan system nighttime data," *Photogram Metric Engineering and Remote Sensing*, vol. 67, no. 9, pp. 1037-1047, 2001.
- [13] D. Lu, *et al.*, "Regional mapping of human settlements in southeastern China with multi sensor remotely sensed data," *Remote Sensing of Environment*, vol. 112, no. 9, pp. 3668-3679, 2008.
- [14] T. Lung, *et al.*, "Human population distribution modelling at regional level using very high resolution satellite imagery," *Applied Geography*, vol. 41, pp. 36-45, 2013.
- [15] M. Langford and D. J. Unwin, "Generating and mapping population density surfaces within a geographical information system," *The Cartographic Journal*, vol. 31, no. 1, pp. 21-26, 1994.
- [16] C. Small, F. Pozzi, and C. D. Elvidge, "Spatial analysis of global urban extent from DMSP-OLS night lights," *Remote Sensing of Environment*, vol. 96, no. 3-4, pp. 277-291, 2005.
- [17] D. Hillger, *et al.*, "First-light imagery from Suomi NPP VIIRS," *Bulletin of the American Meteorological Society*, vol. 94, no. 7, pp. 1019-1029, 2013.

Copyright © 2020 by the authors. This is an open access article distributed under the Creative Commons Attribution License ([CC BY-NC-ND 4.0](https://creativecommons.org/licenses/by-nc-nd/4.0/)), which permits use, distribution and reproduction in any medium, provided that the article is properly cited, the use is non-commercial and no modifications or adaptations are made.

Jianming Yu was born in Hohhot, China, on May 24, 1987. He received B.S. and M.S. degrees in automation from Inner Mongolia University, Hohhot, China, in 2009 and 2013, respectively. From 2013 to 2018, he was an engineer at the Inner Mongolia Earthquake Administration in Hohhot, China. His main research interests are in the fields of earthquake emergency processing and ArcGIS application on the seismology.